Brain Structure and Function
https://doi.org/10.1007/s00429-022-02539-1

SHORT COMMUNICATION

Presence or absence of a prefrontal sulcus is linked to reasoning performance during child development

Ethan H. Willbrand[1,2] · **Willa I. Voorhies**[1,2] · **Jewelia K. Yao**[3] · **Kevin S. Weiner**[1,2] · **Silvia A. Bunge**[1,2]

Received: 29 March 2022 / Accepted: 5 July 2022

Abstract

The relationship between structural variability in late-developing association cortices like the lateral prefrontal cortex (LPFC) and the development of higher-order cognitive skills is not well understood. Recent findings show that the morphology of LPFC sulci predicts reasoning performance; this work led to the observation of substantial individual variability in the morphology of one of these sulci, the para-intermediate frontal sulcus (pimfs). Here, we sought to characterize this variability and assess its behavioral significance. To this end, we identified the pimfs in a developmental cohort of 72 participants, ages 6–18. Subsequent analyses revealed that the presence or absence of the ventral component of the pimfs was associated with reasoning, even when controlling for age. This finding shows that the cortex lining the banks of sulci can support the development of complex cognitive abilities and highlights the importance of considering individual differences in local morphology when exploring the neurodevelopmental basis of cognition.

Keywords Neuroanatomy · Neurodevelopment · Brain imaging · Sulcal pattern · Cortical folding · Prefrontal cortex · Reasoning

Introduction

A major interest in cognitive neuroscience is to understand how variability in brain structure relates to individual differences in complex cognition. Of the many cortical features to study, one of the most prominent is the patterning of the indentations or sulci. While the majority of sulci are identifiable across individuals, some tertiary sulci that emerge late in gestation are not (Chiavaras and Petrides 2000; Lopez-Persem et al. 2019; Amiez et al. 2019; Voorhies et al. 2021; Willbrand et al. in press). For example, the variable presence of the paracingulate sulcus in the anterior cingulate cortex is related to performance on cognitive, motor, and affective tasks in young adults (Fornito et al. 2004, 2006; Whittle et al. 2009; Huster et al. 2009, 2011; Buda et al. 2011; Amiez et al. 2018), inhibitory control in children (Cachia et al. 2014; Borst et al. 2014), and in disorders such as schizophrenia (Yücel et al. 2002, 2003; Le Provost et al. 2003), obsessive–compulsive disorder (Shim et al. 2009), and frontotemporal dementia (Harper et al. 2022). Additional recent work also shows that (i) sulci are missing in the orbitofrontal cortex in individuals with schizophrenia or autism spectrum disorder (Nakamura et al. 2020), and (ii) the absence of multiple sulci in the ventromedial prefrontal cortex (PFC) affects the functional organization of the default mode network (Lopez-Persem et al. 2019). However, it is presently unknown whether the presence or absence of tertiary sulci in the lateral prefrontal cortex (LPFC) impacts cognition in child development.

For example, in a recent study (Voorhies et al. 2021), we demonstrated that the depth of specific LPFC tertiary sulci was related to abstract reasoning ability or the ability to solve novel problems. We observed pronounced variability in the number of components, and overall prominence, of one of the three sulci identified by the model (para-intermediate frontal sulcus, pimfs). Here, we build on this observation by testing the targeted hypothesis that the presence

Kevin S. Weiner and Silvia A. Bunge: shared senior authorship.

✉ Kevin S. Weiner
kweiner@berkeley.edu

[1] Department of Psychology, University of California Berkeley, Berkeley, CA 94720, USA

[2] Helen Wills Neuroscience Institute, University of California Berkeley, Berkeley, CA 94720, USA

[3] Princeton Neuroscience Institute, Princeton University, Princeton, NJ 08540, USA

Published online: 06 August 2022

or absence of specific components of the pimfs, and/or the prominence—quantified as the total sulcal surface area—of this sulcus was related to reasoning abilities. To do so, we investigated the relationship between the variability of the pimfs and relational reasoning scores in a sample of 72 children and adolescents aged 6–18.

Materials and methods

Participants

The present study consisted of 72 typically developing participants between the ages of 6 and 18 (mean ± std age = 12.11 ± 3.77 years old, including 30 individuals identified by caregivers as female) that were randomly selected from the Neurodevelopment of Reasoning Ability (NORA) dataset (Wendelken et al. 2011, 2016, 2017; Ferrer et al. 2013). All participants were right-handed; for additional demographic and socioeconomic information see Supplementary Table 1. In total, 61 of these participants were also included in prior research on sulcal depth (Voorhies et al. 2021). All participants were screened for neurological impairments, psychiatric illness, history of learning disability, and developmental delay. All participants and their parents gave their informed assent/consent to participate in the study, which was approved by the Committee for the Protection of Human Participants at the University of California, Berkeley.

Data acquisition

Imaging data

MRI data were collected on a Siemens 3 T Trio system at the University of California Berkeley Brain Imaging Center. High-resolution T1-weighted MPRAGE anatomical scans (TR = 2300 ms, TE = 2.98 ms, 1 × 1 × 1 mm voxels) were acquired for cortical morphometric analyses.

Behavioral data

All 72 participants completed a matrix reasoning task (WISC-IV), which is a widely used measure of abstract, nonverbal reasoning (Ferrer et al. 2013; Wendelken et al. 2016, 2017). Two additional control measures were included when available: processing speed ($N = 71$) and verbal working memory ($N = 64$). Reasoning performance was measured as a total raw score from the WISC-IV matrix reasoning task (Wechsler 1949; mean ± std = 25.65 ± 6.01). Matrix reasoning is an untimed subtest of the WISC-IV in which participants are shown colored matrices with one missing quadrant. The participant is asked to "complete" the matrix by selecting the appropriate quadrant from an array of options. Previous factor analysis in this dataset (Ferrer et al. 2013) showed that the matrix reasoning score loaded strongly onto a reasoning factor that included three other standard reasoning assessments consisting of the *Block Design* subtest of the Wechsler Abbreviated Scale of Intelligence (WASI; Wechsler 1999), as well as the *Analysis Synthesis* and *Concept Formation* subtests of the Woodcock-Johnson Tests of Achievement (Woodcock et al. 2001).

Processing speed was computed from raw scores on the Cross Out task from the Woodcock-Johnson Psychoeducational Battery-Revised (WJ-R; (Brown et al. 2012)). In this task, the participant is presented with a geometric figure on the left followed by 19 similar figures. The participant places a line through each figure that is identical to the figure on the left of the row. Performance is indexed by the number of rows (out of 30 total rows) completed in 3 min (mean ± std = 22.1 ± 6.75). Cross Out scores are frequently used to estimate processing speed in developmental populations (McBride-Chang and Kail 2002; Kail and Ferrer 2007).

Verbal working memory was measured via raw scores of the Digit Span task from the 4th edition of the Wechsler Intelligence Scale for Children (WISC-IV; Wechsler 1949). The Digits Forward condition of the Digit Span task taxes working memory maintenance, whereas the Backward condition taxes both working memory maintenance and manipulation. In Digits Forward, the experimenter reads aloud a sequence of single-digit numbers, and the participant is asked to immediately repeat the numbers in the same order; in Digits Backward, they are asked to immediately repeat the numbers in the reverse order. The length of the string of numbers increases after every two trials. The Forwards task has eight levels, progressing from 2 to 9 digits. The Backwards task has seven levels, from 2 to 8 digits. Participants are given a score of 1 for a correct answer or a 0 for an incorrect answer. Testing on a given task continues until a participant responds incorrectly to both trials at a given level, after which the experimenter recorded a score out of 16 for Digits Forward (16 total trials; mean ± std = 9.03 ± 2.24) and a score out of 14 for Digits Backward (14 total trials; mean ± std = 5.84 ± 2.12).

Morphological analyses

Cortical surface reconstruction

All T1-weighted images were visually inspected for scanner artifacts. FreeSurfer's automated segmentation tools (Dale et al. 1999; Fischl and Dale 2000; FreeSurfer 6.0.0) were used to generate cortical surface reconstructions. Each anatomical T1-weighted image was segmented to separate gray from white matter, and the resulting boundary was used to reconstruct the cortical surface for each participant (Dale

et al. 1999; Wandell et al. 2000). Each reconstruction was visually inspected for segmentation errors, and these were manually corrected when necessary.

Cortical surface reconstructions facilitate the identification of shallow tertiary sulci compared to post-mortem tissue for two main reasons. First, T1 MRI protocols are not ideal for imaging vasculature; thus, the vessels that typically obscure the tertiary sulcal patterning in post-mortem brains are not imaged on standard resolution T1 MRI scans. Indeed, indentations produced by these smaller vessels that obscure the tertiary sulcal patterning are visible in freely available datasets acquired at high field (7 T) and micron resolution (100–250 µm; Lüsebrink et al. 2017; Edlow et al. 2019). Thus, the present resolution of our T1s (1 mm isotropic) is sufficient to detect the shallow indentations of tertiary sulci but is not confounded by smaller indentations produced by the vasculature. Second, cortical surface reconstructions are made from the boundary between gray and white matter; unlike the outer surface, this inner surface is not obstructed by blood vessels (Weiner et al. 2018; Weiner 2019).

Defining the presence and prominence of the para-intermediate frontal sulcus

We first manually defined the pimfs within each individual hemisphere in *tksurfer* (Miller et al. 2021b). Manual lines were drawn on the *inflated* cortical surface to define sulci based on the most recent schematics of pimfs and sulcal patterning in LPFC by Petrides (Petrides 2019), as well as by the *pial* and *smoothwm* surfaces of each individual (Miller et al. 2021b). In some cases, the precise start or end point of a sulcus can be difficult to determine on a surface (Borne et al. 2020). Thus, using the *inflated*, *pial*, and *smoothwm* surfaces of each individual to inform our labeling allowed us to form a consensus across surfaces and clearly determine each sulcal boundary. For each hemisphere, the location of the pimfs was confirmed by three trained independent raters (E.H.W., W.I.V., J.K.Y.) and finalized by a neuroanatomist (K.S.W.). Although this project focused on a single sulcus, it took the manual identification of all LPFC sulci (2448 sulcal definitions across all 72 participants) to ensure the most accurate definitions of the pimfs components (for descriptions of these LPFC sulci see: Petrides 2019; Miller et al. 2021a, b; Voorhies et al. 2021; Yao et al. 2022).

Individuals typically have three to five tertiary sulci within the middle frontal gyrus (MFG) of the lateral prefrontal cortex (Miller et al. 2021a, b; Voorhies et al. 2021; Yao et al. 2022). The posterior MFG contains three of these sulci, which are present in all participants: the anterior (pmfs-a), intermediate (pmfs-i), and posterior (pmfs-p) components of the posterior middle frontal sulcus (pmfs; Miller et al. 2021a, b; Voorhies et al. 2021; Yao et al. 2022). In contrast, the tertiary sulcus within the anterior MFG, the para-intermediate frontal sulcus (pimfs), is variably present. A given hemisphere can have zero, one, or two pimfs components (Fig. 1A; Supplementary Fig. 1; Voorhies et al. 2021; Yao et al. 2022).

Drawing from criteria outlined by Petrides (2013, 2019), the dorsal and ventral components of the para-intermediate frontal sulcus (pimfs-d and pimfs-v) were generally defined using the following twofold criterion: (i) the sulci ventrolateral to the horizontal and ventral components of the intermediate frontal sulcus, respectively, and (ii) superior and/or anterior to the mid-anterior portion of the inferior frontal sulcus. Note that in this schematic (Petrides 2019), there is presently an unidentified sulcus located on the MFG between the pmfs-a and pimfs-d, which appears as a posterior branch of the imfs-h (below the star (*) symbol in the schematic). In the present work, we included this un-identified sulcus as the posterior extent of the imfs-h in our definitions of the imfs-h. In our sulcal definitions, our principled criteria always identified the pimfs-d below the imfs-h and the pimfs-v always below the imfs-v. Thus, with this criterion, the posterior component of the imfs-h was not confusable with our definition of the pimfs-d. Future work can seek to clarify the incidence and distinctiveness of this branch from the imfs-h. The location of each indentation was cross-checked using the *inflated*, *pial*, and *smoothwm* surfaces. We first confirmed the accuracy of this criterion by applying it to the individual participants with two identifiable pimfs. Next, we extended this criterion to label the cases in which an individual only had one component. We then compared incidence rates between components and hemispheres with a Chi-squared and Fischer exact test, respectively.

We quantified the prominence of the pimfs as its surface area (in mm^2). The surface area values for each pimfs label were extracted using the *mris_anatomical_stats* function that is included in FreeSurfer (Fischl and Dale 2000). For those with two pimfs components, the surface area was extracted as a sum of both components together (via a merged label with *mris_mergelabel* function (Dale et al. 1999)) and for each individual component separately. We also considered normed values. To normalize pimfs surface area by the surface area of the PFC, we automatically defined the PFC in both hemispheres of each participant with the *mris_annot-2label –lobesStrict* function and then extracted surface area values with the *mris_anatomical_stats* function (Fischl and Dale 2000).

Behavioral analyses

Relating the presence of the pimfs to reasoning performance

To assess whether the presence of the pimfs in each hemisphere is related to reasoning performance, we first

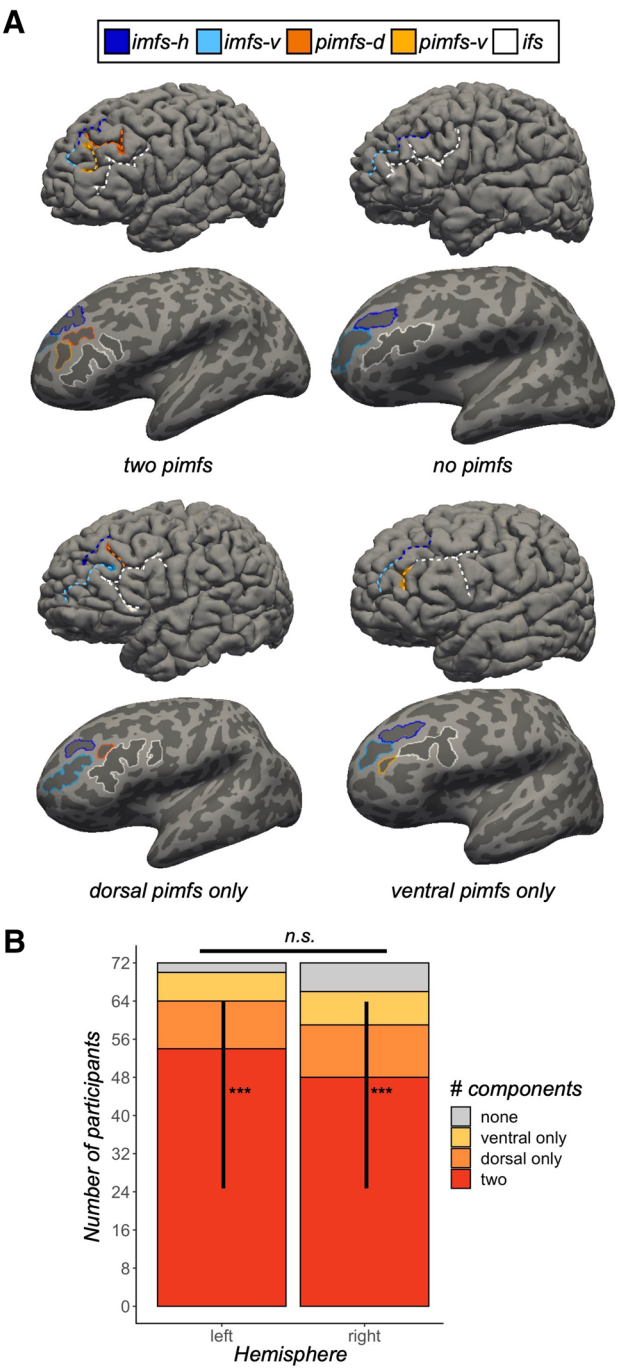

Fig. 1 The para-intermediate frontal sulcus: A tertiary sulcus in lateral prefrontal cortex with pronounced individual differences. **A** Pial (top) and inflated (bottom) left hemispheres (sulci: dark gray; gyri: light gray; cortical surfaces are not to scale) depicting the four types of the para-intermediate frontal sulcus (pimfs): (i) both components present, (ii) neither present, (iii) dorsal component present, (iv) ventral component present. The prominent sulci bounding the pimfs are also shown: the horizontal (imfs-h) and ventral (imfs-v) intermediate frontal sulci and inferior frontal sulcus (ifs). These four sulci are colored according to the legend. **B** Stacked bar plot depicting the incidence of the pimfs components in both hemispheres across the sample ($N = 72$ participants). The incidence of the pimfs is highly variable. In each hemisphere, it is more common for participants to have two components than a single component or no component (***$ps < 0.0001$); the distribution of incidence does not differ between hemispheres ($p = 0.30$). When only one component was present in a given hemisphere, it was equally likely to be a dorsal or ventral component ($ps > 0.30$)

conducted an analysis of covariance (ANCOVA) with number of components in the left and right hemispheres (*two or less than two*) as factors and assessment age as a covariate. There was not a robust relationship between age and the number of pimfs components (*left:* $p = 0.059$, *right*: $p = 0.31$; Supplementary Fig. 2A). Sex was not associated with either matrix reasoning ($p = 0.65$) or the number of components (*left*: $p = 0.27$, *right*: $p = 0.80$), and including sex as a factor in the ANCOVA did not affect the model results, or result in any effects with sex ($ps > 0.44$). Therefore, sex was dropped from the final model. Next, to determine whether the presence of a specific pimfs component was related to reasoning performance, we ran a second ANCOVA with left and right hemisphere presence of the pimfs-v and pimfs-d (*yes, no*) as factors and age as a covariate. Although age differed as a function of the presence/absence of one of the four pimfs components in one hemisphere (left pimfs-d: $p = 0.021$; all other $ps > 0.20$; Supplementary Fig. 2B), this collinearity did not, according to the conventional variance inflation factor (VIF) threshold of five (James et al. 2014), affect the model results (VIF < 2). Further, there were no sex differences in the presence/absence of pimfs components ($ps > 0.37$), and including sex as a factor in the second ANCOVA did not affect the model results, or result in any effects with sex ($ps > 0.75$). Therefore, sex was dropped from the final model.

Control behavioral analyses

To ascertain whether the relationship between left pimfs-v presence and cognition is specific to reasoning performance, or generalizable to other general measures of cognitive processing (Kail and Ferrer 2007), we tested this sulcal-behavior relationship with two other widely used measures of cognitive functioning: processing speed and working memory maintenance and manipulation. Specifically, we ran three ANCOVAs with left pimfs-v presence (*yes, no*) as a factor and assessment age as a covariate.

Matching analysis

To confirm that differences in the sample size and age distribution did not drive the effect of left pimfs-v presence on reasoning scores, we conducted variable-ratio matching on age (ratio = 3:1, min = 1, max = 5) with the *MatchIt* package in R (https://cran.r-project.org/web/packages/MatchIt/MatchIt.pdf). The optimal ratio parameter was determined based on the calculation provided by (Ming and Rosenbaum 2000). To accommodate variable-ratio matching, the

distance between each member of each group was computed by a logit function:

$$Estimate\ \pi_i = Pr\left(noPimfs_i = 1|X\right) = \frac{1}{1 + e^{-X_i\beta}}$$

$$Distance\left(X_i, X_j\right) = \pi_i - \pi_j$$

where X is participant age in groups without (*i*) and with (*j*) a $pimfs_{lh\_ventral}$. Matches were determined by greedy nearest-neighbor interpolation such that each participant in the smaller group received at least one, and up to five, unique matches from the larger group.

A weighted linear regression was then run in the matched sample with left pimfs-v presence and age as predictors of reasoning to confirm the robustness of our initial finding with the whole sample. We then employed a two-pronged analysis to assess and verify the unique variance explained by left pimfs-v presence, while accounting for age-related effects on reasoning. First, we ran a Chi-squared test to compare the previously described weighted-regression model to a weighted-regression model with age only. Second, as described and implemented in prior work (Voorhies et al. 2021; Yao et al. 2022), we fit these two weighted-regression models with leave-one-out cross-validation (looCV), which is suitable for our sample size. Since these are nested models (the largest model contains all elements in the smaller models), the best fit was determined as the model with the lowest cross-validated $RMSE_{cv}$ and the highest R^2_{cv} value.

Relating the size of the pimfs to reasoning performance

To test whether the prominence (surface area) of the pimfs was related to reasoning performance, we implemented a multiple linear regression with surface area of pimfs (combined if two were present) in left and right hemispheres as predictors, while controlling for assessment age. Sex was not included, as it was not related to surface area in either hemisphere (*left*: $p = 0.16$, *right*: $p = 0.78$), and including sex as a factor in the regression did not affect the model results and did not uncover any effects involving sex ($ps > 0.53$). Despite there being a significant correlation between age and left pimfs SA ($r = 0.24$, $p = 0.042$; Supplementary Fig. 2C) and a trending correlation between age and right pimfs SA ($r = 0.20$, $p = 0.087$; Supplementary Fig. 2C), this collinearity did not affect the model results (VIFs < 5); thus, age and left and right pimfs SA were included in the model. As in the previous analysis, we first compared the pimfs SA model to age alone with a Chi-squared test and then further validated with looCV and repeated K-fold (fivefold, 10 repeats) cross-validation methods. Finally, to assess whether prefrontal surface area affected the model, we also ran an exploratory linear regression with normed surface area of the pimfs (by hemispheric PFC surface area) in left and right hemispheres with the covariate assessment age as predictors. See the Supplementary Materials for an in-depth description of these results.

Statistical tests

All statistical tests were implemented in R v4.1.2 (https://www.r-project.org/). Incidence Chi-squared tests were carried out with the *chisq.test* function from the R *stats* package. Fisher's exact tests were carried out with the *fisher.test* function from the R *stats* package. All ANCOVAs were implemented using the *lm* and *Anova* functions from the R *stats* and *cars* packages. Effect sizes for the ANCOVA effects are reported with the *generalized* eta-squared (η2G) metric. Linear models were run using the *lm* function from the R *stats* package. Leave-one-out and K-fold cross-validation analyses were carried out with the *train.control* and *train* functions from the R *caret* package. The effect of each pimfs model was compared to the effect of age alone with the *anova* function from the R *stats* package.

Results

Sulci were manually identified as component(s) of the pimfs in each hemisphere according to previous work (Fig. 1A; Supplementary Fig. 1; Amiez and Petrides 2007; Petrides 2019; Voorhies et al. 2021). We confirmed our prior observation that the pimfs was highly variable (Fig. 1B): in a given hemisphere, there could be zero (*left* = 2.78% of participants; *right* = 8.33%), one (*left:* 22.22%; *right:* 25%), or two components (*left*: 75%; *right:* 66.67%; *left:* $X^2 = 60.333$, $df = 2$, $p < 0.001$; *right:* $X^2 = 39$, $df = 2$, $p < 0.001$; no hemispheric asymmetry: $p = 0.30$). Based on published criteria (Petrides 2013), we further defined pimfs components as either dorsal (pimfs-d) or ventral (pimfs-v) and assessed the prevalence of each component (Fig. 1B). Numerically, a single dorsal component was more frequent than a single ventral one, but statistically these profiles were equally frequent ($X^2 \geq 0.89$, $p > 0.30$ for both hemispheres).

We ran an analysis of covariance (ANCOVA), including age as a covariate, to test the effect of pimfs incidence rates on reasoning task performance (see "Materials and methods" for details on the task). This analysis revealed that the presence of two pimfs components in the left hemisphere was associated with better reasoning performance relative to one or none ($F(1,67) = 4.18$, $p = 0.045$, $\eta_G^2 = 0.059$; Fig. 2A, left). This result was not obtained for the right hemisphere ($F(1,67) = 2.63$, $p = 0.11$, $\eta_G^2 = 0.038$). An ANCOVA testing whether the incidence of a dorsal and/or ventral pimfs component, specifically, was linked to reasoning revealed that the presence of the left hemisphere pimfs-v was associated with

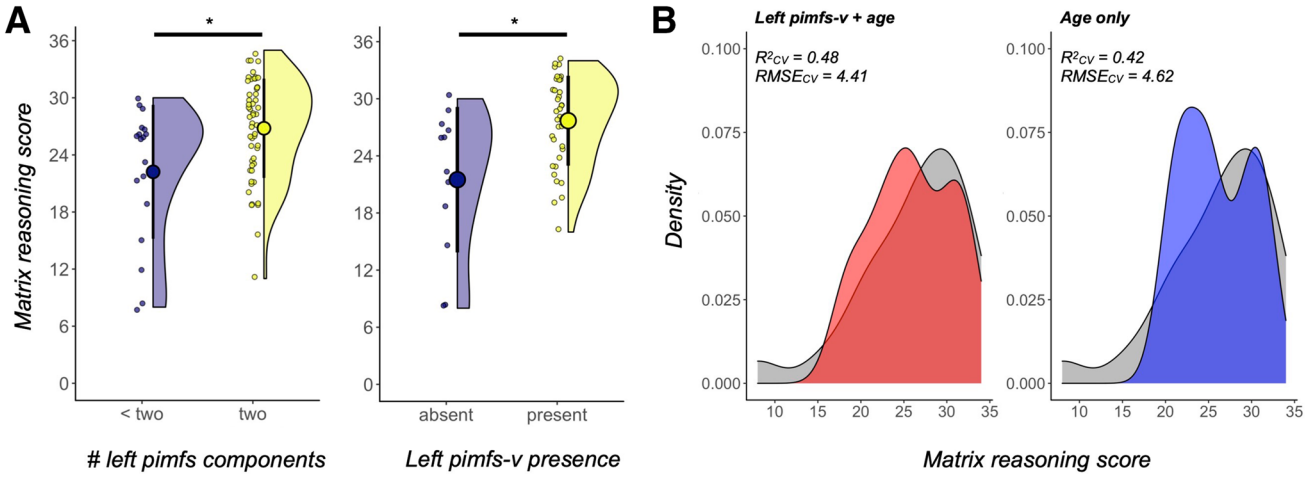

Fig. 2 The presence/absence of the para-intermediate frontal sulcus is related to reasoning. **A** Raincloud plots (Allen et al. 2021) depicting reasoning score as a function of (left) the number of para-intermediate frontal sulcus (pimfs) components and (right) the presence of the ventral pimfs component in the left hemisphere only. The large dots and error bars represent the mean ± std reasoning score, and the violin plots show the kernel density estimate. The smaller dots indicate individual participants. *Left:* Across the whole sample ($N = 72$), those with two pimfs components ($N = 54$) had better reasoning scores than those with only one component ($N = 18$), controlling for age ($^*p = 0.045$). *Right*: Matching subsamples for age and sample size (total $N = 48$), participants with the left pimfs-v component had better reasoning performance than those without, also controlling for age ($^*p = 0.012$); this group difference was also observed across the full sample (Supplementary Fig. 3). **B** Density plots of cross-validated model fit, using leave-one-out cross-validation. *Left:* The predicted scores from the pimfs-v sulcal-behavioral model (visualized in 2A, right; left pimfs-v presence + age) are shown in red and overlaid on the distribution of measured matrix reasoning scores (gray). *Right:* The same format as the left, but for the distribution of predicted scores for the cross-validated nested model with age only (blue). Cross-validated model fit (R^2_{CV}) and root-mean-squared error ($RMSE_{CV}$) are reported for each model. The model including left pimfs-v presence as a factor performs better than the nested model with age alone

higher reasoning scores, controlling for age ($F(1,66) = 5.10$, $p = 0.027$, $\eta_G^2 = 0.072$; Supplementary Fig. 3). Follow-up analyses with additional behavioral measures revealed that the presence of the left pimfs-v was not related to processing speed or phonological working memory (all $ps > 0.50$; see "Materials and methods" for details on the tasks), suggesting some degree of specificity in this brain–behavior relation.

Due to differences in the sample size and age distribution of the two groups ($\text{median(sd)}_{\text{present}} = 11.78(3.52)$, $\text{median(sd)}_{\text{absent}} = 8.81(4.22)$), we sought to further confirm the effect of presence/absence of the left pimfs-v on reasoning performance. To this end, we employed variable-ratio matching ("Materials and methods") to create an age-matched sample that consisted of the original 12 participants without a left pimfs-v and the 36 age-matched participants with a left pimfs-v (mean age = 10.66, eCDF). A weighted regression in the matched sample with left pimfs-v presence and age as predictors of reasoning revealed that the presence of the left pimfs-v remained significant ($\beta = 3.69$, $t = 2.61$, $p = 0.012$; Fig. 2A, right). Critically, this model explained significantly more variance than a model with age alone in the same sample (pimfs: $R_{adj}^2 = 0.51$, $p < 0.001$; age: $R_{adj}^2 = 0.45$, $p < 0.001$; model comparison: $p = 0.012$). We also employed leave-one-out cross-validation to further evaluate the fit of the sulcal-behavioral model relative to the alternative model with age alone ("Materials and methods"). The model including left pimfs-v presence as a factor showed increased prediction accuracy and decreased $RMSE_{CV}$ ($R_{CV}^2 = 0.48$, $RMSE_{CV} = 4.41$; Fig. 2B, left) compared to a model with age only ($R_{CV}^2 = 0.42$, $RMSE_{CV} = 4.62$; Fig. 2B, right), indicating that the presence or absence of the left pimfs-v explained unique variance in reasoning scores above and beyond age.

Finally, in line with previous neuroanatomical analyses (e.g. see Cachia et al. 2018), we examined a continuous metric as a complement to the discrete measure of the presence or absence of a sulcus: total pimfs surface area (mm^2). Left pimfs surface area was correlated with reasoning scores ($\beta = 0.01$, $t = 2.35$, $p = 0.022$; Supplementary Fig. 4). However, total surface area varied as a function of number of components; therefore, we sought to pit the discrete and continuous measures against one another to see whether one provided greater explanatory power. In contrast to the discrete model, the model with pimfs surface area explained reasoning scores only marginally better than age alone ($p = 0.071$; see Supplementary Materials for additional information). Thus, the presence or absence of pimfs-v was more closely linked to reasoning than was total pimfs surface area.

Discussion

Our results reveal that the presence of the left pimfs-v was associated with better reasoning performance in a developmental cohort (6–18 years old). This finding contributes to mounting evidence that the presence or absence of sulci relates to complex cognitive skills (Fornito et al. 2004, 2006; Whittle et al. 2009; Huster et al. 2009, 2011; Buda et al. 2011; Cachia et al. 2014; Borst et al. 2014; Amiez et al. 2018). Crucially, this relationship was not observed for processing speed or working memory, which are theorized to support this high-level cognitive ability (Fry and Hale 2000; Ferrer et al. 2013). Relatedly, we have recently found that the depth of numerous PFC sulci in the left hemisphere—but not the pimfs—is related to working memory manipulation (Yao et al. 2022). Thus, this brain–behavior relationship does not generalize to another challenging cognitive task. It should also be noted that this result was observed across a large developmental age range (6–18 years old). Future work should seek to determine whether this effect holds longitudinally and into adulthood (Huster et al. 2009, 2011; Borst et al. 2014)—or whether this relationship is specific to the time period when higher-level cognitive skills are being acquired.

Relating to previous work, the pimfs-v appears to co-localize with a functionally defined region named rostrolateral PFC, a region that has been implicated in reasoning (e.g. Christoff et al. 2001; Vendetti and Bunge 2014; Urbanski et al. 2016; Hartogsveld et al. 2018; Assem et al. 2020). Anatomically, activation preferentially related to reasoning has been reported to lie along the borders of Brodmann areas (BA) 10/46 and/or 10/47, although precise localization has been impeded by normalization and group averaging of fMRI activation, as well as the emergence of newer anatomical parcellation schemes that subdivide anterior PFC in other ways (e.g. Bludau et al. 2014). Given that the pimfs shows pronounced individual variability, is related to reasoning, and is tentatively located around the border of BA 10/46 (Supplementary Fig. 5), the presence or absence of this indentation could be a novel factor that helps to explain individual variability in the site of task-related activation and/or cytoarchitectural boundaries. However, confirmation of this association awaits individual-level analysis of overlap between pimfs-v, cytoarchitecture, and task-related activation. Considering that the presence of sulci has also been shown to influence the organization of functional networks and task-related activation (Amiez et al. 2013; Amiez and Petrides 2014; Lopez-Persem et al. 2019), future work should also test whether variations in pimfs incidence are related to functional network organization, as well as task-related activation in LPFC.

The sulcal metrics examined here showed significant effects for left pimfs on reasoning skills, with trend-level effects in the right hemisphere. Conversely, we previously showed that sulcal depth of right but not left pimfs (averaged across dorsal and ventral components) was related to reasoning (Voorhies et al. 2021). Both hemispheres have been implicated in reasoning, although there is evidence for functional dissociations between them (Bunge et al. 2009; Vendetti et al. 2015; Goel 2019). The reason for this hemispheric double dissociation is not yet clear; perhaps it relates to differential developmental trajectories of, and dynamic relations between, the two hemispheres (Toga and Thompson 2003), which can be further explored in future research.

Mechanistically, differences in sulcal patterning are hypothesized to be related to the underlying white matter connectivity, and broadly speaking, cortical folding patterns are generally optimized with regard to efficiency of communication between brain regions (Van Essen 1997, 2020; White et al. 2010; Zilles et al. 2013). Thus, the presence and prominence of the pimfs may result in more efficient neural communication compared to the absence of the pimfs. Additionally, or alternatively, relationships among tertiary sulci, brain function, and behavior could relate to alterations of local cytoarchitecture (Amiez et al. 2021). Individual differences in the presence and prominence of tertiary sulci in association cortices may reflect variability in the rates of growth of adjacent cytoarchitectural regions (e.g. Fernández et al. 2016). Thus, the presence or absence of the pimfs could also reflect differences in local architecture which could, in turn, represent differences in local neural circuits reflecting local computational power supporting reasoning—a multiscale, mechanistic relationship that can be explored in future research.

In conclusion, we have uncovered that the presence of a specific sulcus in LPFC may contribute to the development of reasoning. These findings do not imply a deterministic relationship, for two reasons. First, other neuroanatomical features in LPFC and elsewhere have also been linked to reasoning during development, including sulcal depth (Voorhies et al. 2021), white matter microstructure (Wendelken et al. 2017), and, in some samples, cortical thickness (e.g. Leonard et al. 2019). Thus, a goal of future research is to work toward developing a comprehensive, unifying model that integrates these and any other neuroanatomical features, yet to be identified, that contribute to the development of reasoning. The second reason we do not mean to suggest that the presence or absence of this sulcus determines reasoning ability is that there is evidence of experience-dependent plasticity in reasoning and underlying brain circuitry (e.g. Mackey et al. 2013). Nonetheless, the present findings underscore the behavioral relevance of cortical folding patterns, providing novel insights into one particular LPFC sulcus that exhibits prominent individual differences.

Supplementary Information The online version contains supplementary material available at https://doi.org/10.1007/s00429-022-02539-1.

Acknowledgements This research was supported by NICHD R21HD100858 (Weiner, Bunge), NSF CAREER Award 2042251 (Weiner), and an NSF-GRFP fellowship (Voorhies). Funding for original data collection and curation was provided by NINDS R01 NS057156 (Bunge, Ferrer) and NSF BCS1558585 (Bunge, Wendelken). We thank Emilio Ferrer for their advice on the statistical analyses implemented in this study. We also thank former members of the Bunge laboratory for assistance with data collection and the families who participated in the original study.

Author contributions EHW, WIV, KSW, and SAB designed research; EHW, WIV, JKY, and KSW performed manual sulcal labeling; EHW and WIV analyzed data; EHW, WIV, KSW, and SAB wrote the paper; all authors edited the paper and gave final approval before submission.

Data availability Data used for this project have been made freely available on GitHub (https://github.com/cnl-berkeley/stable_projects/tree/main/PresAbs_Reasoning). Requests for further information or raw data should be directed to the Corresponding Author, Kevin Weiner (kweiner@berkeley.edu).

Declarations

Conflict of interest The authors declare no competing financial interests.

References

Allen M, Poggiali D, Whitaker K et al (2021) Raincloud plots: a multi-platform tool for robust data visualization. Wellcome Open Res 4:63

Amiez C, Neveu R, Warrot D et al (2013) The location of feedback-related activity in the midcingulate cortex is predicted by local morphology. J Neurosci 33:2217–2228

Amiez C, Petrides M (2007) Selective involvement of the mid-dorsolateral prefrontal cortex in the coding of the serial order of visual stimuli in working memory. Proc Natl Acad Sci USA 104:13786–13791

Amiez C, Petrides M (2014) Neuroimaging evidence of the anatomo-functional organization of the human cingulate motor areas. Cereb Cortex 24:563–578

Amiez C, Sallet J, Hopkins WD et al (2019) Sulcal organization in the medial frontal cortex provides insights into primate brain evolution. Nat Commun 10:1–14

Amiez C, Sallet J, Novek J et al (2021) Chimpanzee histology and functional brain imaging show that the paracingulate sulcus is not human-specific. Commun Biol 4:54

Amiez C, Wilson CRE, Procyk E (2018) Variations of cingulate sulcal organization and link with cognitive performance. Sci Rep 8:1–13

Assem M, Glasser MF, Van Essen DC, Duncan J (2020) A domain-general cognitive core defined in multimodally parcellated human cortex. Cereb Cortex 30:4361–4380

Bludau S, Eickhoff SB, Mohlberg H et al (2014) Cytoarchitecture, probability maps and functions of the human frontal pole. Neuroimage 93(Pt 2):260–275

Borne L, Rivière D, Mancip M, Mangin J-F (2020) Automatic labeling of cortical sulci using patch- or CNN-based segmentation techniques combined with bottom-up geometric constraints. Med Image Anal 62:101651

Borst G, Cachia A, Vidal J et al (2014) Folding of the anterior cingulate cortex partially explains inhibitory control during childhood: a longitudinal study. Dev Cogn Neurosci 9:126–135

Brown TT, Kuperman JM, Chung Y et al (2012) Neuroanatomical assessment of biological maturity. Curr Biol 22:1693–1698

Buda M, Fornito A, Bergström ZM, Simons JS (2011) A specific brain structural basis for individual differences in reality monitoring. J Neurosci 31:14308–14313

Bunge SA, Helskog EH, Wendelken C (2009) Left, but not right, rostrolateral prefrontal cortex meets a stringent test of the relational integration hypothesis. Neuroimage 46:338–342

Cachia A, Borst G, Vidal J et al (2014) The shape of the ACC contributes to cognitive control efficiency in preschoolers. J Cogn Neurosci 26:96–106

Cachia A, Roell M, Mangin J-F et al (2018) How interindividual differences in brain anatomy shape reading accuracy. Brain Struct Funct 223:701–712

Chiavaras MM, Petrides M (2000) Orbitofrontal sulci of the human and macaque monkey brain. J Comp Neurol 422:35–54

Christoff K, Prabhakaran V, Dorfman J et al (2001) Rostrolateral prefrontal cortex involvement in relational integration during reasoning. Neuroimage 14:1136–1149

Dale AM, Fischl B, Sereno MI (1999) Cortical surface-based analysis I. Segmentation and surface reconstruction. Neuroimage 9:179–194

Edlow BL, Mareyam A, Horn A et al (2019) 7 Tesla MRI of the ex vivo human brain at 100 micron resolution. Sci Data 6:244

Fernández V, Llinares-Benadero C, Borrell V (2016) Cerebral cortex expansion and folding: what have we learned? EMBO J 35:1021–1044

Ferrer E, Whitaker KJ, Steele JS et al (2013) White matter maturation supports the development of reasoning ability through its influence on processing speed. Dev Sci 16:941–951

Fischl B, Dale AM (2000) Measuring the thickness of the human cerebral cortex from magnetic resonance images. Proc Natl Acad Sci U S A 97:11050–11055

Fornito A, Yücel M, Wood S et al (2004) Individual differences in anterior cingulate/paracingulate morphology are related to executive functions in healthy males. Cereb Cortex 14:424–431

Fornito A, Yücel M, Wood SJ et al (2006) Morphology of the paracingulate sulcus and executive cognition in schizophrenia. Schizophr Res 88:192–197

Fry AF, Hale S (2000) Relationships among processing speed, working memory, and fluid intelligence in children. Biol Psychol 54:1–34

Goel V (2019) Hemispheric asymmetry in the prefrontal cortex for complex cognition. Handb Clin Neurol 163:179–196

Harper L, Lindberg O, Bocchetta M et al (2022) Prenatal gyrification pattern affects age at onset in frontotemporal dementia. Cereb Cortex. https://doi.org/10.1093/cercor/bhab457

Hartogsveld B, Bramson B, Vijayakumar S et al (2018) Lateral frontal pole and relational processing: activation patterns and connectivity profile. Behav Brain Res 355:2–11
Huster RJ, Westerhausen R, Herrmann CS (2011) Sex differences in cognitive control are associated with midcingulate and callosal morphology. Brain Struct Funct 215:225–235
Huster RJ, Wolters C, Wollbrink A et al (2009) Effects of anterior cingulate fissurization on cognitive control during stroop interference. Hum Brain Mapp 30:1279–1289
James G, Witten D, Hastie T, Tibshirani R (2014) An introduction to statistical learning: with applications in R. Springer, New York
Kail RV, Ferrer E (2007) Processing speed in childhood and adolescence: longitudinal models for examining developmental change. Child Dev 78:1760–1770
Leonard JA, Romeo RR, Park AT et al (2019) Associations between cortical thickness and reasoning differ by socioeconomic status in development. Dev Cogn Neurosci 36:100641
Le Provost J-B, Bartres-Faz D, Paillere-Martinot M-L et al (2003) Paracingulate sulcus morphology in men with early-onset schizophrenia. Br J Psychiatry 182:228–232
Lopez-Persem A, Verhagen L, Amiez C et al (2019) The human ventromedial prefrontal cortex: sulcal morphology and its influence on functional organization. J Neurosci 39:3627–3639
Lüsebrink F, Sciarra A, Mattern H et al (2017) T1-weighted in vivo human whole brain MRI dataset with an ultrahigh isotropic resolution of 250 µm. Sci Data 4:170032
Mackey AP, Miller Singley AT, Bunge SA (2013) Intensive reasoning training alters patterns of brain connectivity at rest. J Neurosci 33:4796–4803
McBride-Chang C, Kail RV (2002) Cross-cultural similarities in the predictors of reading acquisition. Child Dev 73:1392–1407
Miller JA, D'Esposito M, Weiner KS (2021a) Using tertiary sulci to map the "cognitive globe" of prefrontal cortex. J Cogn Neurosci 1–18
Miller JA, Voorhies WI, Lurie DJ et al (2021b) Overlooked tertiary sulci serve as a meso-scale link between microstructural and functional properties of human lateral prefrontal cortex. J Neurosci 41:2229–2244
Ming K, Rosenbaum PR (2000) Substantial gains in bias reduction from matching with a variable number of controls. Biometrics 56:118–124
Nakamura M, Nestor PG, Shenton ME (2020) Orbitofrontal sulcogyral pattern as a transdiagnostic trait marker of early neurodevelopment in the social brain. Clin EEG Neurosci 51:275–284
Petrides M (2019) Atlas of the morphology of the human cerebral cortex on the average MNI brain. Academic Press
Petrides M (2013) Neuroanatomy of language regions of the human brain. Academic Press
Shim G, Jung WH, Choi J-S et al (2009) Reduced cortical folding of the anterior cingulate cortex in obsessive-compulsive disorder. J Psychiatry Neurosci 34:443–449
Toga AW, Thompson PM (2003) Mapping brain asymmetry. Nat Rev Neurosci 4:37–48
Urbanski M, Bréchemier M-L, Garcin B et al (2016) Reasoning by analogy requires the left frontal pole: lesion-deficit mapping and clinical implications. Brain 139:1783–1799
Van Essen DC (2020) A 2020 view of tension-based cortical morphogenesis. Proc Natl Acad Sci U S A. https://doi.org/10.1073/pnas.2016830117
Van Essen DC (1997) A tension-based theory of morphogenesis and compact wiring in the central nervous system. Nature 385:313–318
Vendetti MS, Bunge SA (2014) Evolutionary and developmental changes in the lateral frontoparietal network: a little goes a long way for higher-level cognition. Neuron 84:906–917
Vendetti MS, Johnson EL, Lemos CJ, Bunge SA (2015) Hemispheric differences in relational reasoning: novel insights based on an old technique. Front Hum Neurosci 9:55
Voorhies WI, Miller JA, Yao JK et al (2021) Cognitive insights from tertiary sulci in prefrontal cortex. Nat Commun 12:5122
Wandell BA, Chial S, Backus BT (2000) Visualization and measurement of the cortical surface. J Cogn Neurosci 12:739–752
Wechsler D (1999) Wechsler abbreviated scale of intelligence--
Wechsler D (1949) Wechsler Intelligence Scale for Children; manual. 113:
Weiner KS (2019) The Mid-Fusiform Sulcus (sulcus sagittalis gyri fusiformis). Anat Rec 302:1491–1503
Weiner KS, Natu VS, Grill-Spector K (2018) On object selectivity and the anatomy of the human fusiform gyrus. Neuroimage 173:604–609
Wendelken C, Ferrer E, Ghetti S et al (2017) Frontoparietal structural connectivity in childhood predicts development of functional connectivity and reasoning ability: a large-scale longitudinal investigation. J Neurosci 37:8549–8558
Wendelken C, Ferrer E, Whitaker KJ, Bunge SA (2016) Fronto-parietal network reconfiguration supports the development of reasoning ability. Cereb Cortex 26:2178–2190
Wendelken C, O'Hare ED, Whitaker KJ et al (2011) Increased functional selectivity over development in rostrolateral prefrontal cortex. J Neurosci 31:17260–17268
White T, Su S, Schmidt M et al (2010) The development of gyrification in childhood and adolescence. Brain Cogn 72:36–45
Whittle S, Allen NB, Fornito A et al (2009) Variations in cortical folding patterns are related to individual differences in temperament. Psychiatry Res Neuroimaging 172:68–74
Willbrand EH, Parker BJ, Voorhies WI et al (in press) Uncovering a tripartite landmark in posterior cingulate cortex. Sci Adv
Woodcock RW, McGrew KS, Mather N, Others (2001) Woodcock-Johnson III tests of achievement
Yao JK, Voorhies WI, Miller JA, et al (2022) Sulcal depth in prefrontal cortex: a novel predictor of working memory performance. Cereb Cortex bhac173
Yücel M, Stuart GW, Maruff P et al (2002) Paracingulate morphologic differences in males with established schizophrenia: a magnetic resonance imaging morphometric study. Biol Psychiatry 52:15–23
Yücel M, Wood SJ, Phillips LJ et al (2003) Morphology of the anterior cingulate cortex in young men at ultra-high risk of developing a psychotic illness. Br J Psychiatry 182:518–524
Zilles K, Palomero-Gallagher N, Amunts K (2013) Development of cortical folding during evolution and ontogeny. Trends Neurosci 36:275–284